

Article pubs.acs.org/est

Disinfection and Electrostatic Recovery of N95 Respirators by Corona Discharge for Safe Reuse

Sriram S. K S Narayanan, Xudong Wang, Jose Paul, Vladislav Paley, Zijian Weng, Libin Ye,* and Ying Zhong*



Cite This: Environ. Sci. Technol. 2021, 55, 15351-15360



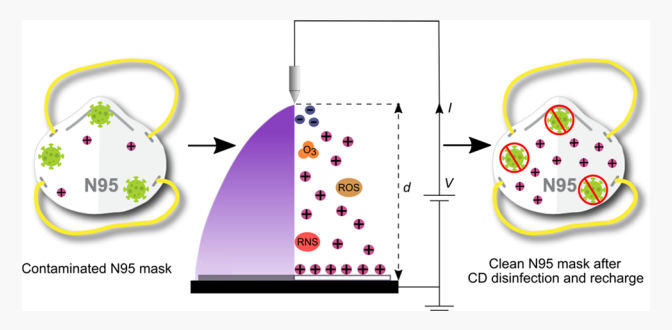
ACCESS I

Metrics & More

Article Recommendations

s Supporting Information

ABSTRACT: With the COVID-19 pandemic surging, the demand for masks is challenging, especially in less-developed areas across the world. Billions of used masks are threatening the environment as a new source of plastic pollution. In this paper, corona discharge (CD) was explored as a safe and reliable method for mask reuse to alleviate the situation. CD can disinfect masks and simultaneously restore electrostatic charges to prevent filtration efficiency deterioration. Electric field, ions, and reactive species generated by CD cause DNA damage and protein denaturation to effectively disinfect N95 respirators. Log reduction of 2-3 against Escherichia coli can be easily reached within 7.5 min. Log reduction of up to 6



can be reached after three cycles of treatment with optimized parameters. CD disinfection is a broad spectrum with log reduction >1 against yeast and >2.5 against spores. N95 respirators can be recharged within 30 s of treatment and the charges can be retained at a higher level than brand-new masks for at least 5 days. The filtration efficiency of masks was maintained at ~95% after 15 cycles of treatment. CD can provide at least 10 cycles of safe reuse with benefits of high safety, affordability, accessibility, and device scalability/portability.

KEYWORDS: COVID-19, N95 masks, corona discharge, disinfection, electrostatic charges

INTRODUCTION

According to the Center of Systems Science and Engineering at Johns Hopkins University, till mid-march 2021, COVID-19 has amassed more than 121 million cases globally and has been attributed to over 2.68 million deaths. 1-3 As filtering facepiece respirators (FFRs) have been confirmed effective for the protection of healthy persons and prevention onward transmission, 4-10 the World Health Organization (WHO) advises the use of FFRs as part of a comprehensive package of prevention and control measures to limit the spread of SARS-CoV-2, the virus that causes COVID-19.11 At the beginning of the COVID-19 pandemic, the U.S. Department of Health and Human Services (HHS) warned of a shortage of hundreds of millions of FFRs.² The value of the global face mask market was \$0.79 billion in 2019, but exploded to an estimated \$166 billion by the end of 2020. 12 As the supply cannot meet the demand, the price of N95s has doubled per the report from Premier, a company that buys medical supplies on behalf of about 40% of U.S. hospitals. 13 One of the major reasons which slow the FFR manufacturing is that, in some countries, surgical masks have to be disinfected by ethylene oxide (ETO) after the manufacturing process. It takes 7-15 days to fully decompose the carcinogenic chemical before the product can be distributed.¹⁴ It is a time, labor, and space-consuming procedure, which limits the supply of FFRs.

By the end of 2020, 52 billion masks were manufactured and about 1.56 billion of them were projected to end up in the oceans. The discarded face masks would further add 8-13 million tons of ocean waste every year, which may take over 450 years to fully decompose. 15 This number keeps growing in 2021. Finding ways to reduce mask use while effectively protecting people from infection is urgent. Limited mask reuse has been approved by the U.S. Centers for Disease Control and Prevention (CDC).¹⁶ A November 2020 survey by the National Nurses United (NNU) reported more than 80% of nurses are still reusing N95 respirators, and their reuse can be up to five shifts or 60 h in most of the hospitals. 17 However, the CDC only listed some "promising" decontamination methods for FFR reuse, including ultraviolet germicidal irradiation (UVGI), vaporous hydrogen peroxide (VHP), and dry heat in April 2020, without obtaining solid data to prove their disinfection efficacy or capability to maintain the 95% filtration efficiency. 16 Healthcare and front-line workers are

Received: April 22, 2021 September 10, 2021 Revised: September 13, 2021 Accepted: Published: September 27, 2021





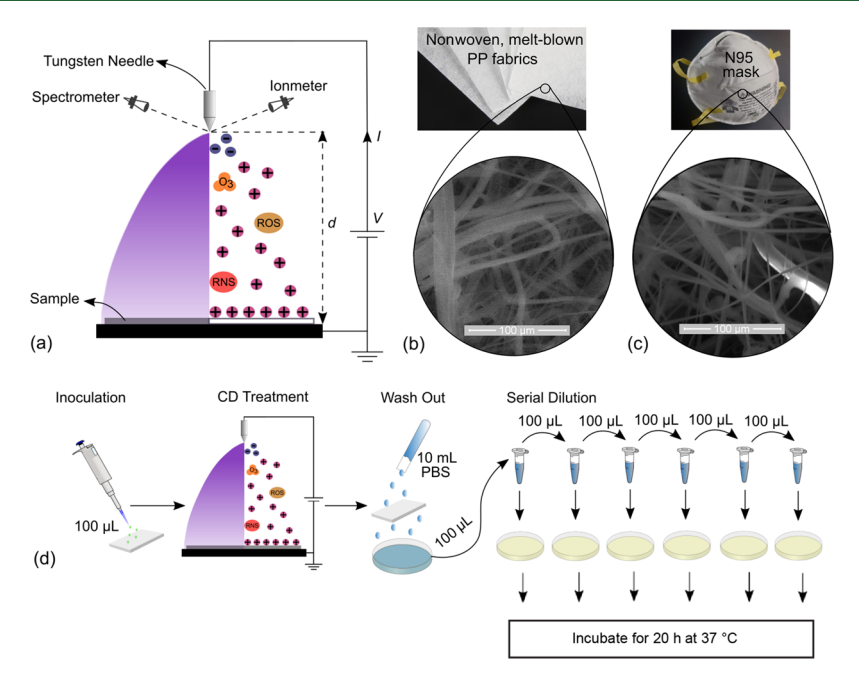


Figure 1. (a) Schematic of the setup applying corona discharge (CD) on target samples. (b, c) Scanning electron microscope (SEM) images of polypropylene (PP) nonwoven fabrics and the filter layer of N95 masks. (d) Procedure of disinfection experiments including inoculation with microorganisms, CD treatment, wash out surviving colonies, serial dilution using phosphate-buffered saline (PBS), plating, and incubation.

concerned about the safety of this reuse. To help address the safety concern, multiple studies have reported the disinfection efficacy of multiple types of disinfection solutions. 18,19 However, some results contradict each other, with some reported ethanol and VHP are the most effective solutions, while others reported dry heating was better.^{21,22} Many of them did not report the particulate filtration efficiency after the disinfection treatment, while some only reported the filtration efficiency result measured by a fit tester,²³ which is far from sufficient to meet the stringent certification tests²⁴ (Procedure No. TEB-APR-STP-0059) established by National Institute of Occupational Safety and Health (NOISH). The disinfection process should not deteriorate any of the filtration mechanisms of FFRs, including inertial impaction, interception, diffusion, and electrostatic attraction. 25-31 Plus, it should not deteriorate the fit between the FFR and the face to minimize the degree of leakage around the facepiece.³² However, UVGI has been reported to cause an increase in aerosol particle penetration, bursting strength, and deteriorated strength of the straps;³³ dry heating and VHP have been reported to cause structural deformation and drop-in fit due to the high temperature needed;²⁰ and alcohol can lead to a drop-in filtration efficiency as much as 43%^{22,34,35} due to the loss of electrostatic charges in FFRs. Therefore, it is urgent to develop a technique which is efficient, convenient, cost-effective, widely applicable, and most importantly not deteriorating to filtration efficiency, for safe reuse of FFRs, to protect both people and the environment.

In this paper, we report the use of corona discharge (CD) as an effective solution to disinfect and electrostatically recharge FFRs simultaneously. Similar to cold plasma, CD is an electrical discharge caused by the ionization of gas surrounding a sharp conductor carrying a high voltage. Most previously reported CD-based disinfection methods such as dielectric barrier discharge (DBD) either require very high power 39-41 (≥50 W) or complex gas flows, 42-45 while the method proposed here can be operated at low power (1.25 W) in an ambient environment without the need for vacuum or

working gases. To validate the capability of CD for safe and efficient FFR disinfection, we evaluated the disinfection and recharging capability of CD for N95 masks and tested the filtration efficiency of N95s using a standard respirator testing procedure (TEB-APR-STP-0059, NIOSH). To guide the practical application of CD, we systematically evaluated the role of each parameter influencing the disinfection efficacy and recharging, explained the disinfection mechanism and identified the damage caused on the DNA and protein of microorganisms.

MATERIALS AND METHODS

Experimental Design. The corona discharge (CD) system was set up as shown in Figure 1a. The voltage and current applied to the discharge needle were controlled by a highvoltage DC power supply (XP Glassman Co. Ltd, FJ Series, 120 W) with a controllable discharge voltage (V) range up to \pm 60 kV and current (I) range up to 0.20 mA. The diameter of the tungsten needle electrode tip for discharge was 1000 μ m compared to 120 μ m for the 5 cm tungsten wire. The polarity of the discharge electrode was set to be positive. The samples were mounted on a stainless-steel stage, which acts as a ground electrode. The needle was set vertically above the sample at a controllable distance pointing to the middle of the sample. CD was applied at atmospheric pressure in an ambient environment (no enclosure, open air) and a closed environment (enclosed in a plexiglass chamber). All experiments were conducted with a low discharge current (I = 0.05 mA) to reduce energy consumption and ensure the safety of the end

To save N95 masks for front-line workers, the samples utilized in our disinfection tests are the nonwoven polypropylene (PP) fabrics used to manufacture FFRs. SEM observation was conducted to compare the microstructure of them with 3M N95 masks (Model: 07048). As indicated in Figure 1b,c, they share similar fiber diameter, density, and

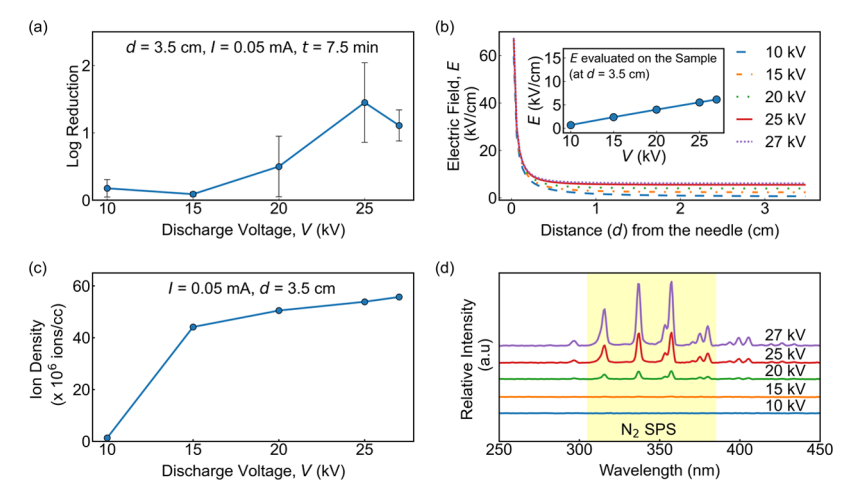


Figure 2. Influence of discharge voltage on (a) Log reduction achieved against *E. coli*. (b) Electric field simulated using COMSOL (inset: as voltage increases, the electric field on the sample increases). (c) Ion density measured using an air ion counter (error bars are insignificant compared to the y values). (d) OES spectrum measured indicating the intensity of N_2 SPS peaks. All results were obtained with discharge parameters set to I = 0.05 mA and d = 3.5 cm.

porosity. Six layers of PP fabrics were stacked together to reach the total thickness of 1.8 mm of an N95 mask. To improve the experimental efficiency, *Escherichia coli* was chosen as the major microorganism in most disinfection tests. As schematized in Figure 1d, the samples were inoculated with $100~\mu\text{L}$ of *E. coli* solution. Then, CD was applied on the samples with controllable parameters, including discharge electrode voltage (V), treatment time (t), electrode—sample distance (d), electrode geometry (needle vs wire), number of treatment cycles (n), and storage time between each cycle (s). Then, the surviving colonies were washed out with phosphate-buffered saline (PBS), followed by serial dilution, culturing, and counting colony forming units (CFU). Log reduction (R) was used as a measure of disinfection efficacy and calculated using eq 1.

$$R = \log(\text{initial colonies}) - \log(\text{surviving colonies})$$
 (1)

To study the effect of treatment time, V and d were set to constants 25 kV and 3.5 cm, respectively, while varying time from t=30 s to 15 min. The effect of electrode—sample distance was investigated by varying d from 2 to 5 cm at V=25 kV for t=7.5 min. To understand the influence of voltage, parameters were set to t=7.5 min and d=3.5 cm, while varying the voltage from V=10 to 27 kV.

Characterization of Corona Discharge. The OES spectrum of CD was acquired using a spectrometer (AvaSpec-ULS2048CL-EVO, Avantes). The fiber optic cable was positioned at a fixed distance of 7.5 cm away from the needle tip (Figure 1a). The ion density from the discharge was measured using an air ion counter (AIC2, α Lab Inc.). The measurements were conducted using positive polarity, and the device was positioned at a parallel distance of 7.5 cm away from the needle tip. Ozone generated due to the combination of molecular and atomic oxygen³⁶ was measured using an ozone meter (Forensics Detectors, model FD-90A-O3, 0.1% resolution).

Disinfection Effect Evaluation. To evaluate the disinfection effect, nonwoven melt-blown PP fabric samples ($5 \times 5 \times 0.03 \text{ cm}^3$, layered six times to mimic the 1.8 mm thickness of N95 masks) were inoculated with *E. coli* (DH5- α derivative, New England Biolabs Inc.), *Pichia pastoris* SMD1163, and *Geobacillus stearothermophilus*, respectively (see the Supporting

Information for cell culture details). For each experiment, 100 μ L of the freshly prepared culture was added to the sample and spread evenly to form a uniform layer covering the entire area of the fabric, the nonwoven fabric; it was immediately transferred and mounted on the stainless-steel ground plane. CD was applied to the sample with the parameters mentioned above. Then, the samples were transferred to a Petri dish, and the surviving colonies were washed out using 10 mL of PBS. Afterward, 100 μ L of this solution was added to 900 μ L of PBS, and this process was repeated to get six serial dilutions. One hundred microliters of each dilution was smeared onto an agar plate for incubation at 37 °C. After 20 h, the surviving colonies were counted. The log reduction is given by eq 1. All experiments were conducted in triplicate.

Plasmid DNA Culture and Purification. The plasmid pPIC9K-A2aR was constructed previously by Ye et al. 46 The plasmids were then amplified and purified (according to GenElute Plasmid Miniprep Kit, Sigma-Aldrich) prior to treatment with CD. The Supporting Information provides details on DNA gel electrophoresis.

Expression and Purification of sfGFP. sfGPF was expressed using arabinose inducible plasmid pBad-sfGFP (AddGene). The sfGFP gene was codon-optimized for *E. coli* with a C-terminal 6-His affinity tag. The protein was purified using TALON Metal Affinity Resin (Takara Bio, Inc.). The Supporting Information provides more details and sodium dodecyl sulfate (SDS) page for electrophoresis.

Recharge Effect Evaluation. Commercially available N95 respirators (3M 8210) were exposed to CD using V=25 kV, I=0.05 mA, and d=3.5 cm. Samples were handled with utmost care to prevent charge accumulation due to environmental effects. After treatment, the surface potential of the top layer of N95 respirators was monitored at three different locations using an electrostatic field meter (FMSX-004, SIMCO Ion). The measurements were taken at a distance of 2.5 cm away from the sample surface at constant intervals starting from 30 min and continuing for 5 days after treatment. The surface charge density (σ_s) is then calculated by solving the Poisson equation. 23,47 In addition, the samples were stored in a humidity-controlled chamber (FSDCBLK100b, FORSPARK), where the relative humidity was maintained between 45 and 60% over the period of observation. All experiments were

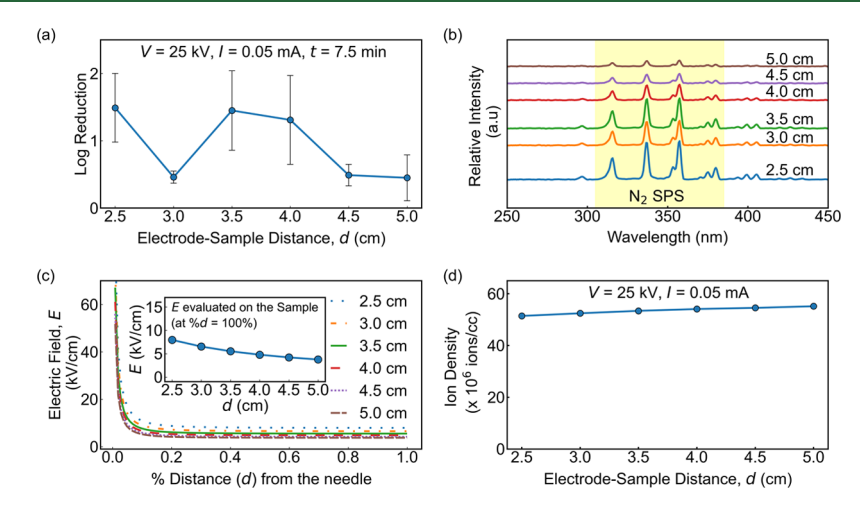


Figure 3. Influence of electrode-sample distance on (a) Log reduction achieved against E. coil. (b) OES spectrum measured indicating N2 SPS peaks. (c) Electric field simulated using COMSOL (inset: as electrode-sample distance is increased, the electric field on the sample reduces). (d) Ion density measured using an air ion counter (error bars are insignificant compared to the y values). All results were obtained with discharge parameters set to V = 25 kV and I = 0.05 mA.

conducted in triplicate using new control samples in pristine condition each time.

Filtration Efficiency Test. The samples were subjected to a 1 min loading test derived from a standard testing procedure from the NIOSH standard testing procedure 24 (Procedure No. TEB-APR-STP-0059, conducted by Nelson Labs), where it was preconditioned at a temperature of 38 ± 2.5 °C and relative humidity of 85 \pm 5% in a controlled ambiance for 25 \pm 1 h, prior to a 1 min load test using NaCl at 85 ± 4 L/min flow rate. The samples were secured on the edges to prevent leakage.

Statistical Analysis. Data are presented as the mean ± standard error. One-way analysis of variance (ANOVA) was used to test the statistical significance of the results presented.

■ RESULTS AND DISCUSSION

Effect of Discharge Voltage (V). Corona can be initiated at ~6 kV in ambient air. However, as indicated in Figure 2a, the voltage of CD must reach higher than 15 kV to obtain a meaningful disinfection effect. The disinfection efficacy increased with voltage, with $R = 0.50 \pm 0.45$ at V = 20 kV and $R = 1.45 \pm 0.59$ at V = 25 kV (with t = 7.5 min and d = 3.5cm). However, the disinfection effect was reduced at V = 27kV, as arcing was observed during the treatment, which limited the area being effectively treated by the CD. The major reasons for the enhanced disinfection efficiency with increasing V can be explained by the increase in the electric field, ion density, and reactive oxygen and nitrogen species (ROS, RNS), which have been reported to be effective for disinfection. 48-53 First, electric fields greater than 5 kV/cm can generate a voltage drop of 1 V across the cell membrane and lead to an electric breakdown of cell walls due to electroporation. 54,55 As shown in Figure 2b, the electric field (E) applied on the sample also increased with voltage, reaching E = 3.96 and 5.52 kV/cm for V = 20 and 25 kV, respectively, meaning that CD can create a strong enough electric field on the microorganisms to play its role in deactivating them.

Second, it has also been reported that the high density of positive and negative ions (between 5×104 and 5×106 ions/ cm³) can cause mechanical damage to cell envelopes.^{50,56} The ion density likewise increased with voltage, reaching 53.87 ×

106 ions/cm³ at V = 25 kV (Figure 2c), which is very effective for disinfection. Figure 2d compares the spectrum intensity generated by CD of different voltages detected by an optical emission spectrometer (OES). It turns out that the intensity of ROS and RNS matched well with the disinfection result, with negligible peaks observed at $V \le 15$ kV and peaks with increased intensity at $V \ge 20$ kV. It has been confirmed that ROS and RNS generated by CD in dry air (which include assemblies of O₃, O₂, O, H₂O₂, NO, NO₂, HNO₃, HNO₂, ONOO-, and OH) can cause oxidative damage in molecular targets leading to DNA, protein, and lipid breakdowns eventually leading to cell death. ^{57–61} The peaks detected in this experiment were mostly at 315.93, 337.13, and 357.69 nm (which belong to the nitrogen second positive system (N₂ SPS)), confirming the presence of RNS. ROS should also have been generated, but they were difficult to be detected as they possess a very short half-life and lose most of their energy colliding with other particles. 51,62,63 However, due to the relatively long half-live of ozone (one type of ROS), ⁶⁴ up to 0.1 ppm was measured using an ozone detector after t = 7.5 min, confirming the generation of ROS. Thus, electric field, ion density, and reactive species all increase with voltage, which can contribute positively to the disinfection efficacy of CD. We plan to decouple the effect of each component on disinfection efficacy in our future experiments.

Effect of Electrode-Sample Distance (d). The strength of the diffuse cone formed by the byproducts of CD and its effective range covered on the sample surface is determined by the electrode to sample electrode-sample distance (d). As indicated in Figure 3a, d must be greater than 3 cm and less than 4.5 cm to obtain meaningful disinfection results. At very short distances, $d \leq 3$ cm, although CD led to a disinfection efficacy of $R = 1.49 \pm 0.51$, it also led to the rise of arcing causing physical damage to the samples. The efficacy increased from $R = 0.46 \pm 0.09$ to 1.45 ± 0.59 and 1.31 ± 0.66 for d = 3, 3.5, and 4 cm, respectively. Hence, between d = 3.5 and 4 cm, the improved disinfection effect may be attributed to an increased size of the inhibition zone (covering the entire 5×5 cm^2 sample) and a strong diffuse cone. At large distances of d≥ 4.5 cm, the strength of the diffuse cone formed by CD becomes weak, leading to a negligible disinfection effect. It matches with the reduction in relative intensity of N₂ SPS

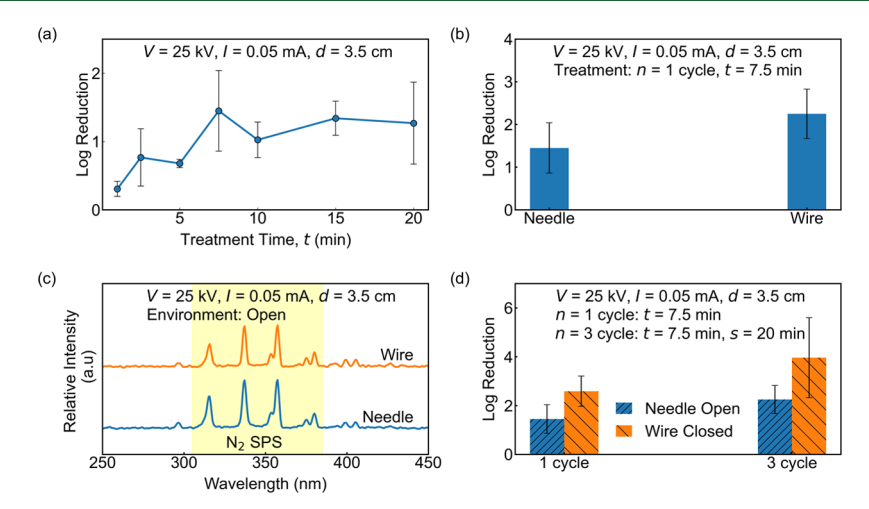


Figure 4. Log reduction achieved (a) with an increase in treatment time (b) with a tungsten needle and a wire. (c) OES spectrum measured indicating N_2 SPS peaks for the needle and wire. (d) Log reduction achieved with introducing treatment cycles in open and closed environments using a needle and a wire, respectively.

peaks observed with the increase of d (Figure 3b), indicating a very weak diffuse cone. The above observation agrees with Warburg's law, which states that the size of the inhibition zone (diffuse cone generated by CD) decreases at shorter distances, while reactive particles (ROS, RNS, and ions) become weaker at larger distances. ^{52,65}

As shown in Figure 3c, the E applied on the sample reached E = 7.94 kV/cm for d = 2.5 cm. With the increase of distance, the electric field reduced from E = 6.52-5.52 kV/cm for d = 3 and 3.5 cm, respectively, before dropping below 5 kV/cm for $d \ge 4$ cm. This trend also matches with the observed log reduction. The ion density remained relatively constant with increasing d, as presented in Figure 3d. It indicates that the increase in disinfection effect is mainly due to the presence of high electric field and reactive species. Therefore, based on the above study, we recommend an optimal electrode—sample distance range of 3.5-4 cm to reach the highest disinfection efficacy of $R = 1.45 \pm 0.59$ against E. coli.

Effect of Treatment Time (t). With V=25 kV and d=3.5 cm, the treatment time was varied from t=1 to 20 min to understand its influence on the disinfection efficacy. Longer exposure to CD led to an increase in disinfection efficacy from $R=0.34\pm0.10$ to 1.56 ± 0.20 for t=1 and 7.5 min, respectively (Figure 4a). The disinfection efficacy could not be significantly increased by further increasing the treatment time to 20 min. Therefore, considering time and energy efficiency, a treatment time of 7.5 min is recommended.

Effect of Electrode Geometry. The geometry of the discharge electrode has a major influence on corona initiation voltage based on Peek's law. ⁶⁶ As shown in Figure 4b, when a tungsten wire (120 μ m diameter, 5 cm length) was used as a discharge electrode, the disinfection efficacy significantly increased to $R=2.25\pm0.57$ compared to 1.45 ± 0.59 (p<0.05), achieved using the tungsten needle (1000 μ m tip diameter, single point discharge). The relative intensities of N_2 SPS peaks observed on the needle and wire electrode were comparable (Figure 4c), but the longer discharge surface of the 5 cm long wire ensured that the entire 5×5 cm² samples were exposed to a stronger and more uniform diffuse cone. Adding treatment cycles and storage time between each cycle leads to improved log reduction (see Figure S1a).

Effect of Cycle Time (n) and Storage Time between Cycles (s). When the sample was moved to a closed environment and treated for n=3 cycles, the disinfection efficacy increased significantly to an average value as high as R=3.96 (Figure 4d), with over three sets (each set includes three samples at least) of experiments reaching R=6 using the tungsten wire as the discharge electrode (Figure S2). It was significantly higher compared to $R=2.59\pm0.62$ using the needle electrode in an open environment (p<0.05). As indicated in Figure S1b, the slower ozone decay inside the closed environment after each treatment cycle ensured consistent exposure to ozone during the treatment phase and storage phase and could be directly responsible for the increased log reduction.

Broad-Spectrum Disinfection. To test the broadspectrum disinfection efficacy of CD, we also conducted disinfection experiments on P. pastoris SMD1163 (a species of methylotrophic yeast) and G. stearothermophilus (which produces heat resistant spores), both of which possess thicker cell walls than E. coli, meaning better tolerance against membrane rupture and DNA leakage. For yeast, a maximum log reduction of 1.04 \pm 0.10 was achieved. For spores, which are more challenging for disinfection in general, log reduction of 2.52 was successfully achieved with three cycles of corona treatment (see the Supporting Information for more details). This indicates that CD can provide broad-spectrum disinfection for different types of microorganisms, including traditionally challenging ones such as spores. In addition, CD is effective for disinfection at most ambient environment of temperatures ranging from 10 to 40 °C and relative humidity varying from 30 to 90%, enabling it for affordable, convenient, and cost-effective broad disinfection applications.

Molecular Mechanism of CD Disinfection. Previous investigations have reported that ROS species were able to induce damage to biomolecules, including DNA and proteins. DNA is a cell's genetic material, and any damage to the DNA may result in changes in encoded proteins, which may lead to malfunctions or complete inactivation of encoded proteins as a consequence of molecular alterations. To evaluate the effectiveness of CD to cause DNA damage, we used plasmid DNA as a starting material and compared its integrity before and after the CD treatment. Twenty microliters of DNA

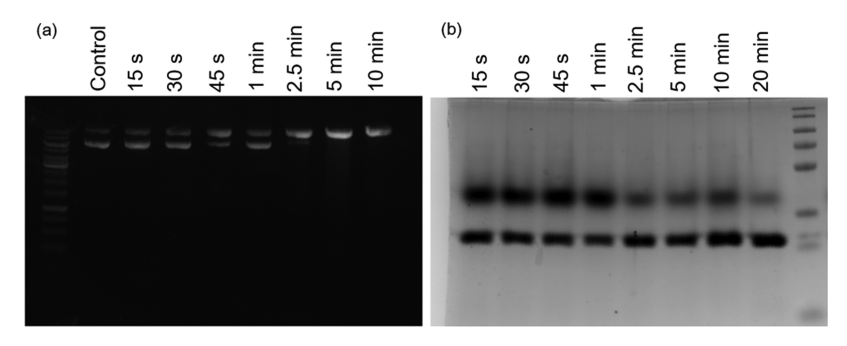


Figure 5. Gel electrophoresis showing bands of (a) DNA plasmids after 15 s to 10 min of exposure to CD. (b) sfGFP protein after 15 s to 20 min of exposure to CD.

plasmids were exposed to CD (at V = 25 kV, d = 3.5 cm and I= 0.05 mA) and analyzed through agarose gel electrophoresis. The treatment time ranged from 15 s to 10 min. Of note, the uncut, undamaged plasmid DNA has two distinct bands (higher and lower bands) on the agarose gel. After damage, the plasmid DNA will be reduced, it to a linear conformation with only one band (higher band) by potentially unfolding a supercoiled form. As shown in Figure 5a, the initiation of DNA breakdown occurred at t = 2.5 min (or between 1 and 2.5 min) and the degradation increased as the CD exposure time prolonged. After 10 min of exposure to CD, all plasmids were in the linearized form. These observations implied that the disinfection of CD could be mediated by breaking the doublestrand DNA. The capability of corona to cause protein damage was investigated by exposing a stable and fluorescent protein to CD. Superfolder green fluorescent protein (sfGFP) is a more robust form of the wide-type GFP (wt-GFP), which shows increased thermal stability and is able to tolerate genetic fusion to poorly folding proteins while remaining fluorescent.⁷ Therefore, observing changes in fluorescence and activation of sfGFP after exposure to CD is of great biological interest. Twenty microliters of sfGFP was exposed to CD (at V = 25kV, d = 3.5 cm, and I = 0.05 mA, t = 15 s to 20 min), then diluted using a PBS (1:5 ratio) before further analysis.

It was observed that the GFP protein starts to break down as well at t = 2.5 min (Figure 5b). As the duration of CD exposure was increased, the proportion of active sfGFP decreased, resulting in approximately complete inactivation. This result clearly revealed that CD as well caused protein damage. While the molecular mechanism of this damage is still unclear, ROS would be one of the most important factors. It may cause modification of proteins in a variety of ways. For example, arginine, lysine, proline, and threonine can be carbonylated; histidine can be modified to oxo-histidine.⁷¹ As a consequence of excessive ROS production, site-specific amino acid modification, fragmentation of the peptide chain, aggregation of cross-linked reaction products, altered electric charge, and increased susceptibility of proteins to proteolysis occur.⁷² Thus, organism inactivation induced by CD has a significant implication for pathogenic sterilization, though further investigations are needed to uncover the molecular level mechanism.

Recharge Effect on N95 Masks (3M 8210). Other than thoroughly disinfect the porous 1.8 mm thick, dielectric, and porous N95 masks, CD can also effectively recover their electrostatic charges. Several studies conclude that incorporating electrostatic charges on FFRs can provide an improved filtration efficiency because of the electrostatic attraction effect. Since most viruses, including SARS-CoV-2, are

negatively charged,⁷⁸ having a net positive charge on the outer surface after treatment could potentially lead to more effective trapping of the virus transported through aerosolized particles. To investigate the recharging effect of CD, N95 respirators were exposed to CD treatments ranging from t=30 s to 10 min, as shown in Figure 6a. After just 30 s of treatment, the

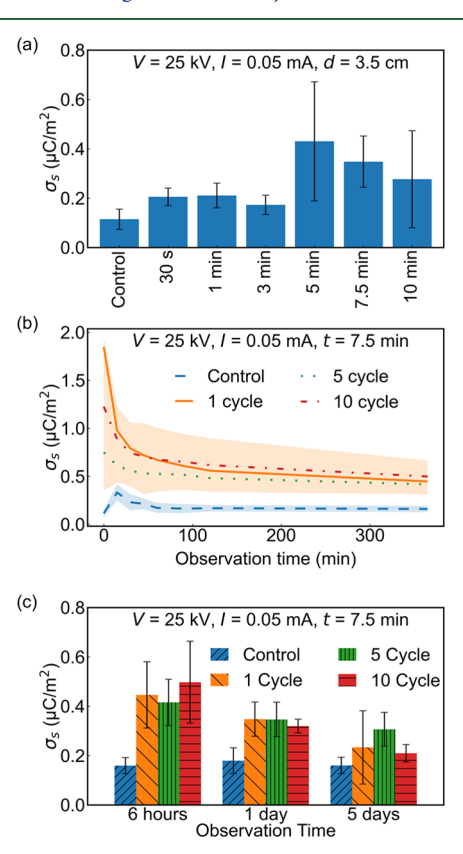


Figure 6. Surface charge density retained (a) with an increase in treatment time from 30 s to 10 min and (b) with an increase in treatment cycles from 1, 5 to 10 cycles, observed within 1 day of treatment and (c) observed after 6 h, 1 day, and 5 days.

surface charge density (σ_s) reached 0.20 \pm 0.03 μ C/m², which was well above that of the control sample $(\sigma_s = 0.11 \pm 0.04 \,\mu$ C/m² with p < 0.05). This indicates that CD can rapidly recover surface charges required to safely restore N95 masks. To study the effect of cyclic CD treatment, full FFR samples were exposed to CD with cycles ranging from n = 1, 5, and 10 cycles. As indicated in Figure 6b, immediately after treatment, σ_s reached as high as $1.84 \pm 0.75 \,\mu$ C/m² after one cycle of CD treatment. It is much higher than the $0.11 \pm 0.04 \,\mu$ C/m²

charge density for untreated control (pristine condition). The charge density decayed very rapidly during the first 150 min of observation right after treatment due to the release and neutralization of extra free surface charges, after which the "injected" charges were retained. This matches our previous observation on bulk polymer films. Even after 5 days of storage, CD-treated samples retained higher charge density of up to $0.34 \pm 0.06 \,\mu\text{C/m}^2$ compared to $0.01 \pm 0.03 \,\mu\text{C/m}^2$ for control samples (p < 0.05), as shown in Figure 6c. This indicates that electrostatic charges recovered by CD in N95 respirators can be retained at a functional level for more than 5 days or even longer. On the contrary, when N95 masks were treated with conventional disinfection methods, surface charges decay rapidly to 52 and 92% of the initial value after exposure to dry heat (at 70 °C) and VHP, respectively. Surface charges decay rapidly to 52 and 92% of the initial value after

As CD can already "fully" recover N95 masks after 30 s (see Figure 6a), increasing the number of treatment cycles for improved disinfection does not influence the recharging effectiveness, as it can be done simultaneously without extra effort. Further, confirmed by SEM observations (see Figure S12), N95 masks subjected to CD did not show signs of physical damage after 10 times of treatment. The CD disinfection is a combined result of exposure to an electric field, ion bombardment, reactive species, and ozone. The low levels of ozone generated by CD (less than 0.1 and 15 ppm in open and closed environments, respectively, for each treatment cycle) are not significant enough to damage the polypropylene melt-blown fibers of N95 masks, allowing CD to be an ideal solution for reuse over several cycles.⁷⁹ Besides N95 masks, CD can also recharge more commonly used face coverings made from natural and synthetic fibers to improve their filtration efficiency.80

Filtration Efficiency Evaluation. Standardized filtration efficiency test (a 1 min loading test derived from NIOSH Procedure No. TEB-APR-STP-0059 using TSI 8130, conducted by Nelson Labs) was performed on N95 respirators subjected to 15 cycles of CD treatment (at V=25 kV, t=7.5 min, s=20 min, in a closed environment, using a 5 cm long tungsten wire electrode). The resulting filtration efficiency of multiple samples was confirmed to be 94.46 \pm 0.372% (Table S1), which is very close to 95%. This result indicates that even subjected to 15 cycles of CD treatment, the filtration efficiencies of N95s were kept almost the same with the unused ones without deterioration. Ideally, safe reusable times for N95s can easily be extended to over 10 times by CD treatment, which is much more than most other disinfection solutions. 68,81

Novelty and Applications. If CD is utilized as the reuse solution, N95 masks can be safely reused for >10 times. In addition to providing guaranteed protection for users, it also has significant environmental impacts. For individuals, if we assume one person uses one renewed mask per day, one will only consume ~35 new masks per year. It is a reduction of 90% for each user. If we assume that 10% of the population all over the world takes advantage of CD mask reuse technology, there will be 4-5 billion less masks disposed to the environment. It will reduce at least 24 million tons of plastic pollution. The application of CD for mask reuse will also reduce the amount of chemicals used for mask disinfection and avoid their environmental impact. Even though high voltage, V= 25 kV, is required, due to the low current needed, $I \le 0.05$ mA, the actual power consumption of CD is less than 1.25 W. In addition to allowing more than 10 cycles of safe reuse of N95 masks by simultaneous disinfection and static charge restoration, CD can also be used to disinfect all types of surfaces, including complex three-dimensional (3D) structures, through noncontact scanning. Compared to traditional disinfection methods (Table S2), it also possesses the advantages of being a nonthermal, nonchemical, and noncontact method with low power consumption, low cost, and easy accessibility. By utilizing commercial hand-held size highvoltage transformers and power supplies, portable CD devices can be designed and manufactured at low cost, which will provide safe mask reuse solutions for the broader public in an affordable and accessible way. Therefore, CD can be a promising reuse solution to significantly address the global mask shortage problem and protect the environment. Further understanding of CD disinfection mechanism will allow the development of more efficient and safe disinfection solutions.

ASSOCIATED CONTENT

Solution Supporting Information

The Supporting Information is available free of charge at https://pubs.acs.org/doi/10.1021/acs.est.1c02649.

Detailed descriptions of cell cultures, COMSOL simulation setup, gel electrophoresis (including SDS page), and filtration efficiency test; comparison of CD with traditional disinfection methods; effects of cycle time (n) and storage time (s) on log reduction; disinfection efficacy against yeast and spores; SEM images of treated *E. coli* compared with control; filtration efficiency results of N95 masks exposed to 15 cycles of CD as reported from Nelson labs; images of LB plates after incubation showing *E. coli* colonies before and after exposure to CD for various discharge parameters discussed; and SEM images for N95 masks before and after treatment (PDF)

AUTHOR INFORMATION

Corresponding Authors

Libin Ye — Department of Cell Biology, Microbiology and Molecular Biology, University of South Florida, Tampa, Florida 33620, United States; H. Lee Moffitt Cancer Center & Research Institute, Tampa, Florida 33612, United States; orcid.org/0000-0003-0818-2972; Email: libinye@usf.edu

Ying Zhong — Department of Mechanical Engineering, University of South Florida, Tampa, Florida 33620, United States; orcid.org/0000-0002-1845-7127; Email: yingzhong@usf.edu

Authors

Sriram S. K S Narayanan — Department of Mechanical Engineering, University of South Florida, Tampa, Florida 33620, United States; orcid.org/0000-0002-3163-9275

Xudong Wang – Department of Cell Biology, Microbiology and Molecular Biology, University of South Florida, Tampa, Florida 33620, United States

Jose Paul - Department of Mechanical Engineering, University of South Florida, Tampa, Florida 33620, United States

Vladislav Paley – Department of Mechanical Engineering, University of South Florida, Tampa, Florida 33620, United States Zijian Weng - Department of Mechanical Engineering, University of South Florida, Tampa, Florida 33620, United States

Complete contact information is available at: https://pubs.acs.org/10.1021/acs.est.1c02649

Notes

The authors declare no competing financial interest.

ACKNOWLEDGMENTS

This work is supported by the National Science Foundation (#2030033) and COVID-19 Rapid Response Grant supported by University of South Florida. The authors would like to thank Dr. Rob Knight, Dr. Pedro Belda-Ferre and Dr. Shi Huang at University of California at San Diego (UCSD) for their contribution on testing the disinfection efficiency on SARS-CoV-2 virus; Dr. Yu Qiao and Dr. Rui Kou (UCSD) for the equipment and contributions towards improving corona discharge related simulations. The authors would also like to thank the staff at Nanotechnology Research and Education Center (University of South Florida, Tampa) for assisting with SEM imaging of biological samples.

REFERENCES

- (1) Johns Hopkins Coronavirus Resource Center. Covid-19 Map. https://coronavirus.jhu.edu/map.html (accessed Mar 19, 2021).
- (2) Grimm, C. A. Hospital Experiences Responding to the Covid-19 Pandemic: Results of a National Pulse Survey March 23-27, Office of Inspector General; US Department of Health and Human Services,
- (3) Smith-Spark, L. Global Tally of Confirmed Coronavirus Cases Surpasses 100 Million. https://edition.cnn.com/2021/01/26/world/ coronavirus-100-million-cases-intl/index.html (accessed Feb 15, 2021).
- (4) Asadi, S.; Bouvier, N.; Wexler, A. S.; Ristenpart, W. D. The Coronavirus Pandemic and Aerosols: Does Covid-19 Transmit Via Expiratory Particles? Aerosol Sci. Technol. 2020, 54, 635-638.
- (5) Howard, J.; Huang, A.; Li, Z.; Tufekci, Z.; Zdimal, V.; van der Westhuizen, H.-M.; von Delft, A.; Price, A.; Fridman, L.; Tang, L.-H. An Evidence Review of Face Masks against Covid-19. Proc. Natl. Acad. Sci. U.S.A. 2021, 118.
- (6) Leung, N. H.; Chu, D. K.; Shiu, E. Y.; Chan, K.-H.; McDevitt, J. J.; Hau, B. J.; Yen, H.-L.; Li, Y.; Ip, D. K.; Peiris, J. M.; et al. Respiratory Virus Shedding in Exhaled Breath and Efficacy of Face Masks. Nat. Med. 2020, 26, 676-680.
- (7) Peeples, L. Face Masks: What the Data Say. Nature 2020, 586, 186-189.
- (8) Asadi, S.; Cappa, C. D.; Barreda, S.; Wexler, A. S.; Bouvier, N. M.; Ristenpart, W. D. Efficacy of Masks and Face Coverings in Controlling Outward Aerosol Particle Emission from Expiratory Activities. Sci. Rep. 2020, 10, No. 15665.
- (9) Roberge, R. J.; Roberge, M. R. Cloth Face Coverings for Use as Facemasks During the Coronavirus (Sars-Cov-2) Pandemic: What Science and Experience Have Taught Us. Disaster Med. Public Health Preparedness 2020, 1-29.
- (10) Raymond, J. The Great Mask Debate: A Debate That Shouldn't Be a Debate at All. WMJ 2020, 119, 229-239.
- (11) World Health OrganizationMask Use in the Context of Covid-19: Interim Guidance, 1 December 2020; World Health Organization: Geneva, 2020.
- (12) Sharma, M. Covid-19 Hazard: 1.56 Bn Masks Polluted Oceans in 2020, Claims Study. https://www.businesstoday.in/coronavirus/ covid-19-hazard-156-bn-masks-pollute-oceans-in-2020-claims-study/ story/426450.html (accessed Feb 15, 2021).
- (13) Noguchi, Y. Why N95 Masks Are Still in Short Supply in the U.S. https://www.npr.org/sections/health-shots/2021/01/27/

- 960336778/why-n95-masks-are-still-in-short-supply-in-the-u-s (accessed Feb 15, 2021).
- (14) Liteplo, R. G.; Meek, M. E. Concise International Chemical Assessment Document 54; World Health Organization: Geneva, 2003.
- (15) Gupta, A. Tsunami of 1.56 Billion Masks Triggers New Wave of Marine Pollution. https://news.cgtn.com/news/2020-12-08/ Tsunami-of-1-56-billion-masks-triggers-new-wave-of-marinepollution-W3jOBoX5cY/index.html (accessed Feb 15, 2021).
- (16) Centers for Disease Control and Prevention. Implementing Filtering Facepiece Respirator (FFR) Reuse, Including Reuse after Decontamination, When There Are Known Shortages of N95 Respirators. https://www.cdc.gov/coronavirus/2019-ncov/hcp/ppestrategy/decontamination-reuse-respirators.html (accessed Feb 15, 2021).
- (17) National Nurses United National Nurse Survey Exposes Hospitals' Knowing Failure to Prepare for a Covid-19 Surge During Flu Season. https://www.nationalnursesunited.org/press/nationalnurse-survey-4-exposes-hospitals-knowing-failure-prepare-covid-19surge (accessed Feb 15, 2021).
- (18) Viscusi, D. J.; Bergman, M. S.; Eimer, B. C.; Shaffer, R. E. Evaluation of Five Decontamination Methods for Filtering Facepiece Respirators. Ann. Occup. Hyg. 2009, 53, 815-827.
- (19) Bergman, M. S.; Viscusi, D. J.; Heimbuch, B. K.; Wander, J. D.; Sambol, A. R.; Shaffer, R. E. Evaluation of Multiple (3-Cycle) Decontamination Processing for Filtering Facepiece Respirators. J. Eng. Fibers Fabr. 2010, 5, No. 155892501000500405.
- (20) Fischer, R. J.; Morris, D. H.; van Doremalen, N.; Sarchette, S.; Matson, M. J.; Bushmaker, T.; Yinda, C. K.; Seifert, S. N.; Gamble, A.; Williamson, B. N.; et al. Effectiveness of N95 Respirator Decontamination and Reuse against SARS-CoV-2 Virus. Emerging Infect. Dis. 2020, 26, 2253.
- (21) Oh, C.; Araud, E.; Puthussery, J. V.; Bai, H.; Clark, G. G.; Wang, L.; Verma, V.; Nguyen, T. H. Dry Heat as a Decontamination Method for N95 Respirator Reuse. Environ. Sci. Technol. Lett. 2020, 7, 677-682.
- (22) Liao, L.; Xiao, W.; Zhao, M.; Yu, X.; Wang, H.; Wang, Q.; Chu, S.; Cui, Y. Can N95 Respirators Be Reused after Disinfection? How Many Times? ACS Nano 2020, 14, 6348-6356.
- (23) Yim, W.; Cheng, D.; Patel, S. H.; Kou, R.; Meng, Y. S.; Jokerst, J. V. Kn95 and N95 Respirators Retain Filtration Efficiency Despite a Loss of Dipole Charge During Decontamination. ACS Appl. Mater. Interfaces 2020, 12, 54473-54480.
- (24) NIOSH Personal Protective Equipment information (PPE Info). Procedure No. Teb-Apr-Stp-0059. https://wwwn.cdc.gov/ PPEInfo/Standards/Info/TEBAPRSTP0059 (accessed Mar 10,
- (25) Centers for Disease Control and Prevention. N95 Respirators and Surgical Masks. https://blogs.cdc.gov/niosh-science-blog/2009/ 10/14/n95/ (accessed Feb 15, 2021).
- (26) Steinberg, B. E.; Aoyama, K.; McVey, M.; Levin, D.; Siddiqui, A.; Munshey, F.; Goldenberg, N. M.; Faraoni, D.; Maynes, J. T. Efficacy and Safety of Decontamination for N95 Respirator Reuse: A Systematic Literature Search and Narrative Synthesis. Can. J. Anaesth. 2020, 67, 1814-1823.
- (27) Tcharkhtchi, A.; Abbasnezhad, N.; Seydani, M. Z.; Zirak, N.; Farzaneh, S.; Shirinbayan, M. An Overview of Filtration Efficiency through the Masks: Mechanisms of the Aerosols Penetration. Bioact. Mater. 2021, 6, 106-122.
- (28) Zangmeister, C. D.; Radney, J. G.; Vicenzi, E. P.; Weaver, J. L. Filtration Efficiencies of Nanoscale Aerosol by Cloth Mask Materials Used to Slow the Spread of SARS-CoV-2. ACS Nano 2020, 14, 9188-
- (29) Lin, T. H.; Chen, C. C.; Huang, S. H.; Kuo, C. W.; Lai, C. Y.; Lin, W. Y. Filter Quality of Electret Masks in Filtering 14.6-594 Nm Aerosol Particles: Effects of Five Decontamination Methods. PLoS One 2017, 12, No. e0186217.
- (30) Huang, S. H.; Chen, C. W.; Kuo, Y. M.; Lai, C. Y.; McKay, R.; Chen, C. C. Factors Affecting Filter Penetration and Quality Factor of Particulate Respirators. Aerosol Air Qual. Res. 2013, 13, 162-171.

- (31) Lin, T. H.; Tseng, C. C.; Huang, Y. L.; Lin, H. C.; Lai, C. Y.; Lee, S. A. Effectiveness of N95 Facepiece Respirators in Filtering Aerosol Following Storage and Sterilization. *Aerosol Air Qual. Res.* **2020**, *20*, 833–843.
- (32) Centers for Disease Control and Prevention. Healthcare Respiratory Protection Resources. https://www.cdc.gov/niosh/npptl/hospresptoolkit/fittesting.html (accessed Feb 15, 2021).
- (33) Lindsley, W. G.; Martin, S. B., Jr.; Thewlis, R. E.; Sarkisian, K.; Nwoko, J. O.; Mead, K. R.; Noti, J. D. Effects of Ultraviolet Germicidal Irradiation (UVGI) on N95 Respirator Filtration Performance and Structural Integrity. J. Occup. Environ. Hyg. 2015, 12, 509–517.
- (34) Viscusi, D. J.; King, W. P.; Shaffer, R. E. Effect of Decontamination on the Filtration Efficiency of Two Filtering Facepiece Respirator Models. *J. Int. Soc. Respir. Prot.* **2007**, *24*, 93.
- (35) Juang, P. S.; Tsai, P. N95 Respirator Cleaning and Reuse Methods Proposed by the Inventor of the N95 Mask Material. *J. Emerg. Med.* **2020**, *58*, 817–820.
- (36) Chang, J.-S.; Lawless, P. A.; Yamamoto, T. Corona Discharge Processes. *IEEE Trans. Plasma Sci.* **1991**, *19*, 1152–1166.
- (37) Fridman, A.; Chirokov, A.; Gutsol, A. Non-Thermal Atmospheric Pressure Discharges. *J. Phys. D: Appl. Phys.* **2005**, 38, No. R1.
- (38) Goldman, M.; Goldman, A.; Sigmond, R. The Corona Discharge, Its Properties and Specific Uses. *Pure Appl. Chem.* **1985**, 57, 1353–1362.
- (39) Aziz, K. H. H.; Miessner, H.; Mahyar, A.; Mueller, S.; Kalass, D.; Moeller, D.; Omer, K. M. Removal of Dichloroacetic Acid from Aqueous Solution Using Non-Thermal Plasma Generated by Dielectric Barrier Discharge and Nano-Pulse Corona Discharge. Sep. Purif. Technol. 2019, 216, 51–57.
- (40) Laroussi, M.; Alexeff, I.; Kang, W. L. Biological Decontamination by Nonthermal Plasmas. *IEEE Trans. Plasma Sci.* **2000**, 28, 184–188
- (41) Singh, R. K.; Philip, L.; Ramanujam, S. Continuous Flow Pulse Corona Discharge Reactor for the Tertiary Treatment of Drinking Water: Insights on Disinfection and Emerging Contaminants Removal. *Chem. Eng. J.* **2019**, *355*, 269–278.
- (42) Abramzon, N.; Joaquin, J. C.; Bray, J.; Brelles-Mariño, G. Biofilm Destruction by Rf High-Pressure Cold Plasma Jet. *IEEE Trans. Plasma Sci.* **2006**, *34*, 1304–1309.
- (43) Bermúdez-Aguirre, D.; Wemlinger, E.; Pedrow, P.; Barbosa-Cánovas, G.; Garcia-Perez, M. Effect of Atmospheric Pressure Cold Plasma (APCP) on the Inactivation of Escherichia Coli in Fresh Produce. Food Control 2013, 34, 149–157.
- (44) Dobrynin, D.; Friedman, G.; Fridman, A.; Starikovskiy, A. Inactivation of Bacteria Using Dc Corona Discharge: Role of Ions and Humidity. *New J. Phys.* **2011**, *13*, No. 103033.
- (45) Ye, S.-y.; Song, X.-l.; Liang, J.-L.; Zheng, S.-h.; Lin, Y. Disinfection of Airborne Spores of *Penicillium expansum* in Cold Storage Using Continuous Direct Current Corona Discharge. *Biosyst. Eng.* **2012**, *113*, 112–119.
- (46) Ye, L.; Van Eps, N.; Zimmer, M.; Ernst, O. P.; Prosser, R. S. Activation of the a 2a Adenosine G-Protein-Coupled Receptor by Conformational Selection. *Nature* **2016**, 533, 265–268.
- (47) Zhong, Y.; Kou, R.; Wang, M.; Qiao, Y. Electrification Mechanism of Corona Charged Organic Electrets. *J. Phys. D: Appl. Phys.* **2019**, *52*, No. 445303.
- (48) Han, L.; Patil, S.; Boehm, D.; Milosavljević, V.; Cullen, P.; Bourke, P. Mechanisms of Inactivation by High-Voltage Atmospheric Cold Plasma Differ for *Escherichia coli* and *Staphylococcus aureus*. *Appl. Environ. Microbiol.* **2016**, 82, 450–458.
- (49) Liao, X.; Liu, D.; Xiang, Q.; Ahn, J.; Chen, S.; Ye, X.; Ding, T. Inactivation Mechanisms of Non-Thermal Plasma on Microbes: A Review. *Food Control* **2017**, *75*, 83–91.
- (50) Noyce, J.; Hughes, J. Bactericidal Effects of Negative and Positive Ions Generated in Nitrogen on *Escherichia coli. J. Electrost.* **2002**, *54*, 179–187.

- (51) Pai, K.; Timmons, C.; Roehm, K. D.; Ngo, A.; Narayanan, S. S.; Ramachandran, A.; Jacob, J. D.; Ma, L. M.; Madihally, S. V. Investigation of the Roles of Plasma Species Generated by Surface Dielectric Barrier Discharge. *Sci. Rep.* **2018**, *8*, No. 16674.
- (52) Scholtz, V.; Julák, J.; Kříha, V. The Microbicidal Effect of Low-Temperature Plasma Generated by Corona Discharge: Comparison of Various Microorganisms on an Agar Surface or in Aqueous Suspension. *Plasma Processes Polym.* **2010**, *7*, 237–243.
- (53) Sysolyatina, E.; Mukhachev, A.; Yurova, M.; Grushin, M.; Karalnik, V.; Petryakov, A.; Trushkin, N.; Ermolaeva, S.; Akishev, Y. Role of the Charged Particles in Bacteria Inactivation by Plasma of a Positive and Negative Corona in Ambient Air. *Plasma Processes Polym.* **2014**, *11*, 315–334.
- (54) Zimmermann, J.; Shimizu, T.; Schmidt, H.; Li, Y.; Morfill, G.; Isbary, G. Test for Bacterial Resistance Build-up against Plasma Treatment. *New J. Phys.* **2012**, *14*, No. 073037.
- (55) Babaeva, N. Y.; Kushner, M. J. Intracellular Electric Fields Produced by Dielectric Barrier Discharge Treatment of Skin. *J. Phys. D: Appl. Phys.* **2010**, *43*, No. 185206.
- (56) Scholtz, V.; Julák, J.; Kríha, V.; Mosinger, J.; Kopecká, S. Decontamination Effects of Low-Temperature Plasma Generated by Corona Discharge. Part Ii: New Insights. *Prague Med. Rep.* **2007**, *108*, 128–146.
- (57) Dobrynin, D.; Fridman, G.; Friedman, G.; Fridman, A. Physical and Biological Mechanisms of Direct Plasma Interaction with Living Tissue. *New J. Phys.* **2009**, *11*, No. 115020.
- (58) Gaunt, L. F.; Beggs, C. B.; Georghiou, G. E. Bactericidal Action of the Reactive Species Produced by Gas-Discharge Nonthermal Plasma at Atmospheric Pressure: A Review. *IEEE Trans. Plasma Sci.* **2006**, 34, 1257–1269.
- (59) Graves, D. B. The Emerging Role of Reactive Oxygen and Nitrogen Species in Redox Biology and Some Implications for Plasma Applications to Medicine and Biology. *J. Phys. D: Appl. Phys.* **2012**, *45*, No. 263001.
- (60) Moldgy, A.; Nayak, G.; Aboubakr, H. A.; Goyal, S. M.; Bruggeman, P. J. Inactivation of Virus and Bacteria Using Cold Atmospheric Pressure Air Plasmas and the Role of Reactive Nitrogen Species. *J. Phys. D: Appl. Phys.* **2020**, *53*, No. 434004.
- (61) Scholtz, V.; Julák, J.; Kríha, V.; Mosinger, J. Decontamination Effects of Low-Temperature Plasma Generated by Corona Discharge. Part I: An Overview. *Prague Med. Rep.* **2007**, *108*, 115–127.
- (62) Mhamdi, A.; Van Breusegem, F. Reactive Oxygen Species in Plant Development. *Development* **2018**, *145*, No. dev164376.
- (63) Ziuzina, D.; Patil, S.; Cullen, P.; Keener, K.; Bourke, P. Atmospheric Cold Plasma Inactivation of *Escherichia coli* in Liquid Media inside a Sealed Package. *J. Appl. Microbiol.* **2013**, *114*, 778–787
- (64) Pandiselvam, R.; Thirupathi, V. Reaction Kinetics of Ozone Gas in Green Gram (Vigna Radiate). *Ozone: Sci. Eng.* **2015**, *37*, 309–315.
- (65) Sigmond, R. Simple Approximate Treatment of Unipolar Space-Charge-Dominated Coronas: The Warburg Law and the Saturation Current. *J. Appl. Phys.* **1982**, *53*, 891–898.
- (66) Peek, F. W. Visual Corona. In *Dielectric Phenomena in High Voltage Engineering*, 2nd ed.; McGraw-Hill Book Company, Incorporated, 1920; pp 38–78.
- (67) Misra, N.; Moiseev, T.; Patil, S.; Pankaj, S.; Bourke, P.; Mosnier, J.; Keener, K.; Cullen, P. Cold Plasma in Modified Atmospheres for Post-Harvest Treatment of Strawberries. *Food Bioprocess Technol.* **2014**, *7*, 3045–3054.
- (68) Lee, J.; Bong, C.; Lim, W.; Bae, P. K.; Abafogi, A. T.; Baek, S. H.; Shin, Y.-B.; Bak, M. S.; Park, S. Fast and Easy Disinfection of Coronavirus-Contaminated Face Masks Using Ozone Gas Produced by a Dielectric Barrier Discharge Plasma Generator. *Environ. Sci. Technol. Lett.* **2021**, *8*, 339–344.
- (69) Timoshkin, I. V.; Maclean, M.; Wilson, M. P.; Given, M. J.; MacGregor, S. J.; Wang, T.; Anderson, J. G. Bactericidal Effect of Corona Discharges in Atmospheric Air. *IEEE Trans. Plasma Sci.* **2012**, 40, 2322–2333.

- (70) Pédelacq, J. D.; Cabantous, S.; Tran, T.; Terwilliger, T. C.; Waldo, G. S. Engineering and Characterization of a Superfolder Green Fluorescent Protein. *Nat. Biotechnol.* **2006**, *24*, 79–88.
- (71) Ezraty, B.; Gennaris, A.; Barras, F.; Collet, J.-F. Oxidative Stress, Protein Damage and Repair in Bacteria. *Nat. Rev. Microbiol.* **2017**, *15*, 385–396.
- (72) Sharma, P.; Jha, A. B.; Dubey, R. S.; Pessarakli, M. Reactive Oxygen Species, Oxidative Damage, and Antioxidative Defense Mechanism in Plants under Stressful Conditions. *J. Bot.* **2012**, *2012*, No. 217037.
- (73) Barrett, L. W.; Rousseau, A. D. Aerosol Loading Performance of Electret Filter Media. Am. Ind. Hyg. Assoc. J. 1998, 59, 532–539.
- (74) Hossain, E.; Bhadra, S.; Jain, H.; Das, S.; Bhattacharya, A.; Ghosh, S.; Levine, D. Recharging and Rejuvenation of Decontaminated N95 Masks. *Phys. Fluids* **2020**, 32, No. 093304.
- (75) Kilic, A.; Shim, E.; Pourdeyhimi, B. Electrostatic Capture Efficiency Enhancement of Polypropylene Electret Filters with Barium Titanate. *Aerosol Sci. Technol.* **2015**, *49*, 666–673.
- (76) Lee, H. R.; Liao, L.; Xiao, W.; Vailionis, A.; Ricco, A. J.; White, R.; Nishi, Y.; Chiu, W.; Chu, S.; Cui, Y. Three-Dimensional Analysis of Particle Distribution on Filter Layers inside N95 Respirators by Deep Learning. *Nano Lett.* **2021**, 21, 651–657.
- (77) Zhao, M.; Liao, L.; Xiao, W.; Yu, X.; Wang, H.; Wang, Q.; Lin, Y. L.; Kilinc-Balci, F. S.; Price, A.; Chu, L.; et al. Household Materials Selection for Homemade Cloth Face Coverings and Their Filtration Efficiency Enhancement with Triboelectric Charging. *Nano Lett.* **2020**, 20, 5544–5552.
- (78) Michen, B.; Graule, T. Isoelectric Points of Viruses. J. Appl. Microbiol. 2010, 109, 388–397.
- (79) Lerouge, S.; Simmons, A. Sterilisation of Biomaterials and Medical Devices; Elsevier, 2012.
- (80) Sanchez, A. L.; Hubbard, J. A.; Dellinger, J. G.; Servantes, B. L. Experimental Study of Electrostatic Aerosol Filtration at Moderate Filter Face Velocity. *Aerosol Sci. Technol.* **2013**, *47*, 606–615.
- (81) Lee, J.; Bong, C.; Bae, P. K.; Abafog, A. T.; Baek, S. H.; Shin, Y.-B.; Park, M. S.; Park, S.; et al. Fast and Easy Disinfection of Coronavirus-Contaminated Face Masks Using Ozone Gas Produced by a Dielectric Barrier Discharge Plasma Generator. *Environ. Sci. Technol. Lett.* **2021**, *8*, 339–344.